Available online at www.sciencedirect.com

SciVerse ScienceDirect

Ceramics International 38 (2012) 3237–3242

CERAMICS INTERNATIONAL

www.elsevier.com/locate/ceramint

Temperature-dependent electrical properties of B-site zinc substituted bismuth sodium titanate piezoceramics

Hao Zhang [a], Shao-Jie Fu [b], Wei-Jie Long [a], Dong-Jie Guo [a,*]

[a] Institute of Bio-inspired Structure and Surface Engineering, Nanjing University of Aeronautics and Astronautics, Nanjing 210016, China
[b] National Laboratory of Solid State Microstructures, Nanjing University, Nanjing 210093, China

Received 21 November 2011; received in revised form 5 December 2011; accepted 5 December 2011
Available online 19 December 2011

Abstract

Lead-free ceramics of B-site Zn substituted $Bi_{0.5}Na_{0.5}TiO_3$, with the formula of $(1-x)Bi_{0.5}Na_{0.5}TiO_3$–$xBi(Zn_{0.5}Ti_{0.5})O_3$ (BNT–BZT, $x = 0.01$, 0.04, 0.07) have been prepared. These compositions have rhombohedral, rhombohedral–tetragonal morphotropic phase boundary, and tetragonal crystal structure, respectively. The polarization–electric field (*P–E*), bipolar and unipolar strain–electric field (*S–E*) curves of all the compositions are measured as the functions of temperature. The temperature-dependent values of the remnant polarization, maximum polarization, coercive field, bipolar and unipolar strain, as well as the shape change of *P–E* and *S–E* curves have been comparatively investigated and discussed. The observed different temperature-dependences of the above parameters are attributed to the fact that the introduction of BZN reduces the depolarization temperature and enhances relaxor characteristics, which is consistent with the temperature-dependent dielectric properties. These results are valuable in understanding and further designing noval BNT-based lead-free piezoelectric systems with high recoverable strain.

Keywords: C. Electrical properties; Lead-free; BNT–BZT; Temperature-dependence

1. Introduction

Piezoelectric ceramics are widely used in electronic devices such as sensors and actuators [1]. The current materials for such applications are dominantly based on lead-based $Pb(Zr,Ti)O_3$ (PZT) because of the high electrical performance. However, as lead is toxic and PbO can easily take vaporization during the sealing process in high temperature, lead-based materials should be ruled out of commercial applications from the viewpoint of environmental and healthy considerations. Motivated by this goal, great efforts have been devoted to the development of high performance lead-free piezoelectric materials. Perovskite-based oxides such as $Bi_{0.5}Na_{0.5}TiO_3$ (BNT) and $K_{0.5}Na_{0.5}NbO_3$ (KNN)-based solid solutions have been investigated as the possible candidates for high performance lead-free piezoceramics [2,3]. Among these developed systems, the BNT-based one has been widely investigated because of the advantage of easy preparation procedure and good electrical properties [4–7] because the rhombohedral BNT can form morphotropic phase boundaries (MPB) with other lead-free perovskite oxides with different crystal structures such as tetragonal, orthorhombic [4]. It is summarized that there are two classes of MPBs for BNT-based lead free piezoelectric materials, and the first one is that between rhombohedral–tetragonal, which can have high electrical performance in the MPB region [4]. The second class of BNT-based MPBs are usually that between rhombohedral-cubic/pseudocubic structures, which usually do not show significantly improved electrical properties. Among the reported BNT-based MPBs, the recent reported 0.96BNT–0.04$Bi(Zn_{0.5}Ti_{0.5})O_3$ (BNT–BZT) belongs to the first class, which separating rhombohedral–tetragonal structures [8]. In this system, the introduction of BZT decreases the depolarization temperature (T_d), which corresponding to the ferroelectric–antiferroelectric phase transition, and results in enhanced relaxor behavior around T_d of BNT-based solid solutions by disrupt the long range ferroelectric order. Such low-temperature shift of T_d and relaxor behavior usually can lead to weak antiferroelectric order and thus giant recoverable strain [9], which is an important factor for application of piezoelectric

* Corresponding author. Tel.: +86 25 84892584; fax: +86 25 84892581.
E-mail address: djguo@nuaa.edu.cn (D.-J. Guo).

0272-8842/$36.00
doi:10.1016/j.ceramint.2011.12.029

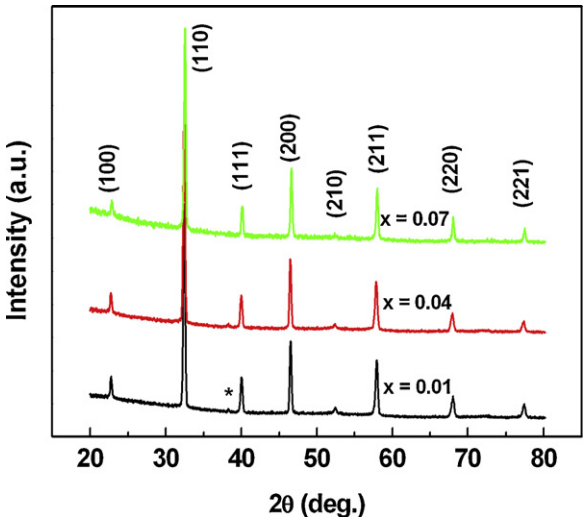

Fig. 1. X-ray diffraction patterns the BNT–BZT ceramic.

ceramics in actuator because the strain energy density is proportional to the square maximum achievable strain (S^2_{max}) [10].

On the other hand, it is noted that piezoelectric devices should be able to work under various conditions and environments such as high temperature region, therefore, it is necessary to evaluate the temperature-dependent electric performance of the materials behavior under high temperatures [11,12]. Motivated by this idea and to further understand the recently reported BNT–BZT system, we investigated the temperature-dependent electrical properties of $(1-x)$BNT–xBZT, where $x = 0.01$, 0.04 and 0.07. These designed compositions go from rhombohedral, rhombohedral–tetragonal MPB, and to tetragonal crystal structure, in other words, these three compositions have rhombohedral, rhombohedral–tetragonal MPB, and tetragonal structure, respectively, according to the report [8].

2. Experimental procedures

BNT–BZT ceramics were prepared by a conventional ceramic fabrication method using Bi_2O_3, Na_2CO_3, ZnO, and TiO_2 with purity higher than 99.0% were chosen as the starting raw materials. The starting materials were weighed stoichiometrically and ball milled for 24 h in ethanol. The dried slurries were calcined at 900 °C for 3 h and then ball milled again for 24 h. The powders were then pressed into disks with a diameter of 10 mm under 70 MPa. Sintering was carried out at 1100 °C in covered alumina crucibles for 3 h.

The crystal structures of the ceramics were characterized by powder X-ray diffraction (XRD, Rigaku Ultima III) using Cu Kα radiation. Electric measurements were carried out on ground sintered disks. The circular surfaces of the disks were covered with a thin layer of silver paint and fired at 550 °C for 30 min. The silver layers served as electrodes. Relative permittivity and loss of fresh ceramics were measured using

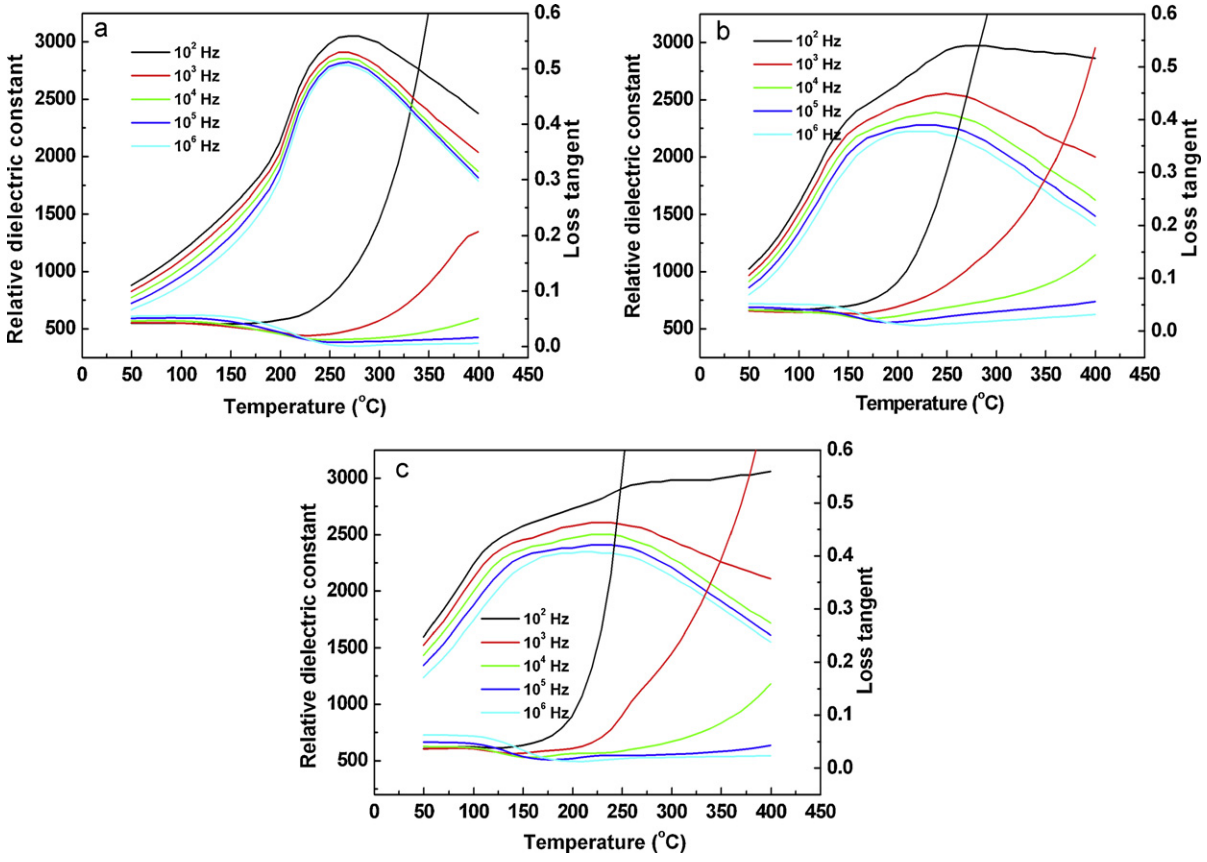

Fig. 2. Temperature-dependent dielectric properties of the BNT–BZT ceramics, showing the decreased T_d by introducing BZT.

an impedance analyzer (HP4284A, Hewlett-Packard Company) at frequencies ranging from 100 Hz to 1 MHz in a temperature range of 50–400 °C. Polarization–electric field (*P–E*), bipolar and unipolar strain–electric field (*S–E*) curves were measured at 1 Hz by Precision premier II (Radiant Tech., USA). The piezoelectric coefficient (d_{33}) and the electromechanical coupling factor (k_p) were measured with a Berlincourt d_{33} meter (ZJ-6A, China) and HP4294A on poled samples, the sample poling was performed by applying an electric field of 6 kV/mm to the samples at room-temperature.

3. Results and discussion

Fig. 1 shows the XRD patterns of the sintered BNT–BZT ceramics. These results show that all the ceramics have a single-phase perovskite structure. The peak of the composition with $x = 0.01$ indicated by a star is attributed to the superstructure of *R3c* space group, indicating the rhombohedral crystal of this composition. With increasing x, this peak tends to disappear, that means its structure changed. According to the report [8], the compositions with $x = 0.01$ and 0.07 have the rhombohedral and tetragonal structures, respectively, while that with $x = 0.04$ lying in the rhombohedral–tetragonal MPB region, which is further confirmed by the piezoelectric measurements. At room temperature, the measured piezoelectric coefficient and coupling factor (d_{33}, k_p) are (68 pC/N, 0.15), (82 pC/N, 0.21) (55 pC/N, 0.12), respectively. These results are comparable with other report [8] on this system and other BNT-based systems [4,13,14].

The relative permittivity (ε_r) and dielectric loss (tan δ) of the BNT-BZT ceramics are measured from 50 °C to 400 °C with different frequencies, as shown in Fig. 2(a)–(c) for the compositions with $x = 0.01$, 0.04, and 0.07, respectively. As can be seen, the peak corresponding to the maximum ε_r tends to be significantly broadened with the increase of BZT content. This result is attributed to the introduce of BZT, which decreases the depolarization temperature (T_d) from around 200 °C to around 100 °C. Meanwile, the introduce of BZT also enhances the relaxor behavior, which is indicated by the frequency dependent ε_r–T and tan δ–T curves and that the phase transitions, no matter from ferroelectric to antiferroelectric (T_d) or from antiferroelectric to paraelectric phase (T_c), show a broadened temperature "peak" [15], as evidenced by the broad ε_r–T and tan δ–T peaks in Fig. 2, the above results are consistent

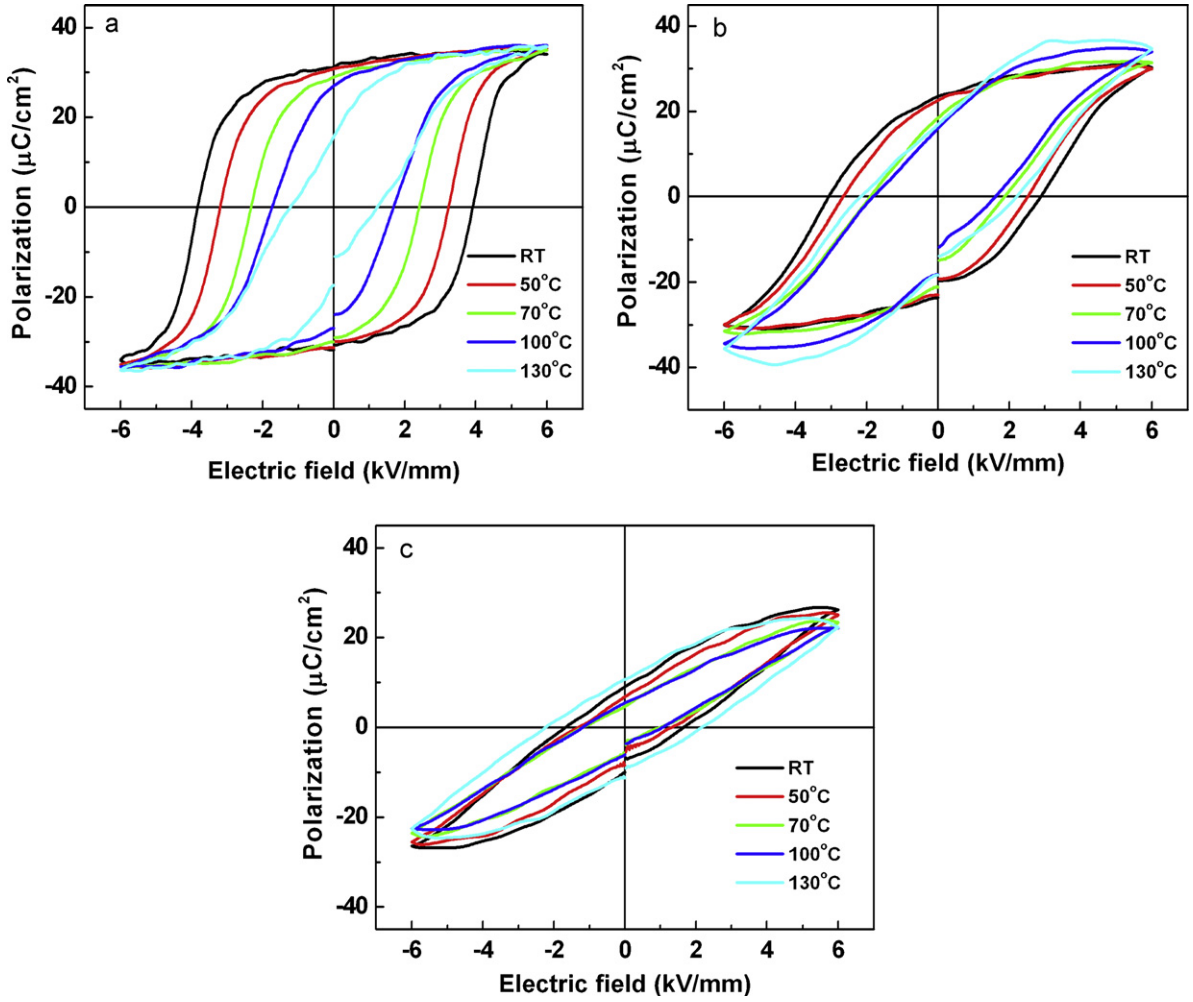

Fig. 3. Temperature-dependent *P–E* hysteresis loops for the compositions with (a) $x = 0.01$, (b) $x = 0.04$, and (c) $x = 0.07$, respectively.

with other reports on BNT-based lead-free piezoceramics [4,8,12,14].

The *P–E* ferroelectric loops were measured with a maximum E-field of 6 kV/mm at different temperatures, as shown in Fig. 3(a)–(c) for the compositions with $x = 0.01$, 0.04, and 0.07, respectively. At a fixed temperature, the *P–E* loops tend to become slim with increasing x, accompanied by decreased remanent polarization (P_r) and maximum polarization (P_{max}), which indicates the weakened ferroelectricity with increasing x and can be attributed to the decreased T_d [8,13], as observed in Fig. 2. For example, at room temperature, the (P_r, P_{max}) are (34.5 μC/cm^2, 31.2 μC/cm^2), (30.2 μC/cm^2, 23.4 μC/cm^2), and (26.3 μC/cm^2, 8.6 μC/cm^2), for the three compositions, respectively.

On the other hand, the composition with $x = 0.01$ shows ferroelectricity in the whole temperature range. However, with increasing temperature, the P_r and the coercive field (E_c) decrease monotonously, whereas the P_{max} keeps almost constant. It is noted that the shape of *P–E* loops changed, e.g., the *P–E* loops become slightly pinched when temperature reaches 130 °C, indicating the possible appearance of weak antiferroelectric order. However, for the other two compositions, the P_r or P_{max} tends to increase when temperature is higher than 100 °C, which may be attributed to the thermal induced high leakage current [12,14].

Fig. 4(a)–(c) plots the temperature-dependent bipolar *S–E* curves. For the composition with $x = 0.01$ and 0.04, the *S–E* curves exhibit a butterfly shape, which confirms the ferroelectric nature of this composition, in the measured temperature range because of its high T_d. This result is consistent with the *P–E* loops shown in Fig. 3(a). It should be noted that with increasing temperature, the maximum strain increases while the ''negative strain'', which denotes the difference between zero field strain and the lowest strain, decreases, this again indicating the possible weak antiferroelectric order. For the other composition with $x = 0.07$, the above mentioned shape change of the bipolar *S–E* curves are not so significantly and the strain values increases firstly and then decreases with increasing temperature, which is due to its lowest T_d. In addition, it can be seen that the ''negative strain'' almost vanishes when temperature reaches 100 °C, close to T_d temperature, which is actually the onset temperature of the antiferroelectric phase. Such results suggest a possible weak antiferroelectric nature at this temperature. Actually, similar results are also observed in

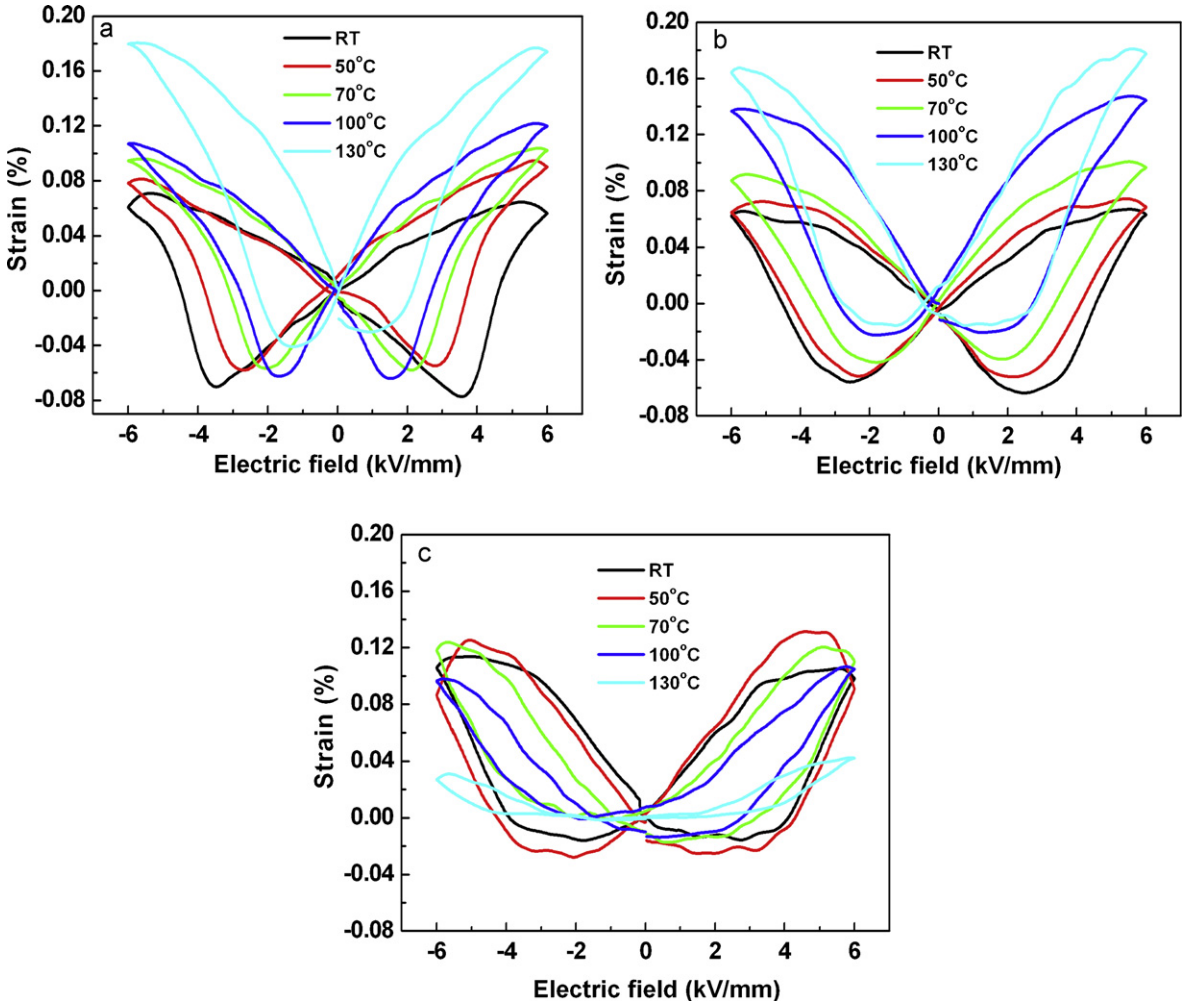

Fig. 4. Temperature-dependent bipolar *S–E* hysteresis loops for the compositions with (a) $x = 0.01$, (b) $x = 0.04$, and (c) $x = 0.07$, respectively.

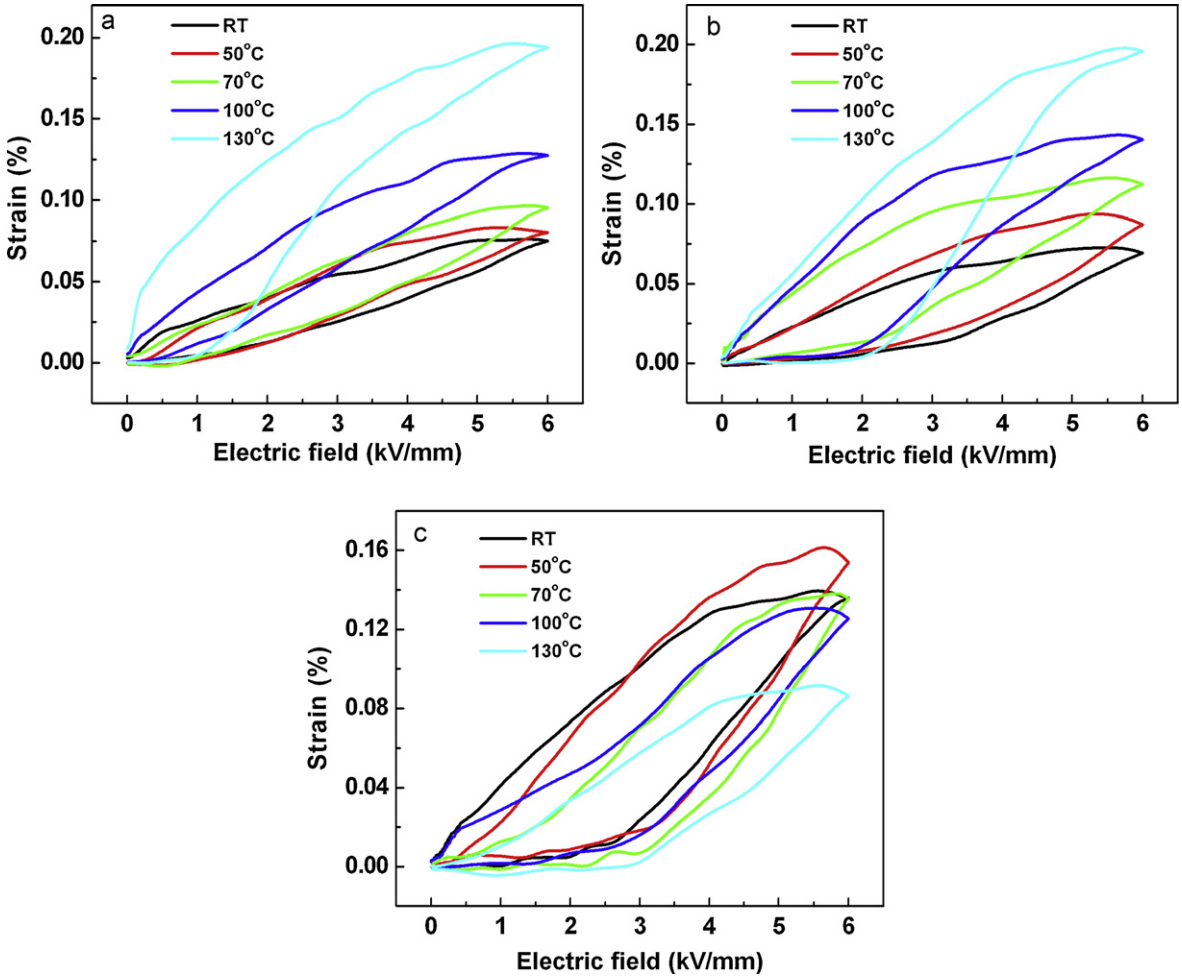

Fig. 5. Temperature-dependent unipolar *S–E* hysteresis loops for the compositions with (a) $x = 0.01$, (b) $x = 0.04$, and (c) $x = 0.07$, respectively.

lead-based antiferroelectric ceramics and BNT-based single crystal and ceramics [8,10,16–18].

Fig. 5(a)–(c) shows the temperature-dependent unipolar *S–E* curves for these compositions, respectively. In general, Fig. 5 clearly demonstrates the decreased T_d with increasing BZT content by comparing the temperature-dependent shape change of the unipolar *S–E* curves. In detail, the compositions with $x = 0.01$ and 0.04 have the similar temperature-dependence of the unipolar *S–E* curves, i.e., the strain value increases monotonously with increasing temperature [12,14] and the maximum values of both compositions can reach 0.19%. However, for the composition with $x = 0.07$, the strain values increases firstly and then decreases with increasing temperature, consistent with the temperature-dependence of the bipolar strain.

4. Conclusions

In summary, lead-free ceramics of BNT-BZT with $x = 0.01$, 0.04, 0.07 have been prepared and investigated. It is found that the introduction of BZT results in decreased T_d and enhanced relaxor behavior, which is responsible for the observed different temperature-dependence of P_r, P_{max}, E_c, and S values, as well as the *P–E*, bipolar and unipolar *S–E* curve shapes. The maximum recoverable unipolar strain can be reached 0.19% for the compositions with $x = 0.04$. Our results may be helpful for understanding temperature-dependent properties of BNT-based lead-free piezoelectric systems.

Acknowledgements

This work was supported by National Natural Science Foundation No. 50805076, Science Research Foundation at NUAA no. NS2012014, National Natural Science Key Corporation Foundations Nos. 60910007 and 61161120323.

References

[1] G.H. Haertling, Ferroelectric ceramics: history and technology, J. Am. Ceram. Soc. 82 (1999) 797–818.
[2] S.J. Zhang, R. Xia, T.R. Shrout, Lead-free piezoelectric ceramics: alternatives for PZT? J. Electroceram. 19 (2007) 51–57.
[3] I.-H. Chan, C.-T. Sun, M.-P. Houng, S.-Y. Chu, Sb doping effects on the piezoelectric and ferroelectric characteristics of lead-free $Na_{0.5}K_{0.5}Nb_{1-x}Sb_xO_3$ piezoelectric ceramics, Ceram. Int. 37 (2011) 2061–2068.
[4] Y. Hiruma, H. Nagata, T. Takenaka, Detection of morphotropic phase boundary of $(Bi_{1/2}Na_{1/2})TiO_3$–$Ba(Al_{1/2}Sb_{1/2})O_3$ solid-solution ceramics, Appl. Phys. Lett. 95 (2009) 052903.

[5] Y.W. Liao, D.Q. Xiao, D.M. Lin, J.G. Zhu, P. Xu, L. Wu, X.P. Wang, Synthesis and properties of $Bi_{0.5}(Na_{1-x-y}K_xAg_y)_{0.5}TiO_3$ lead-free piezoelectric ceramics, Ceram. Int. 33 (2007) 1445–1448.
[6] C.Y. Kim, T. Sekino, K. Niihara, Synthesis of bismuth sodium titanate nanosized powders by solution/sol–gel process, J. Am. Ceram. Soc. 86 (2003) 1464–1467.
[7] S. Trujillo, J. Kreisel, Q. Jiang, J.H. Smith, P.A. Thomas, P. Bouvier, F. Weiss, The high pressure behavior of Ba-doped $Bi_{1/2}Na_{1/2}TiO_3$ investigated by Raman spectroscopy, J. Phys. Condens. Matter 17 (2005) 6587–6597.
[8] S.T. Zhang, B. Yang, F. Yan, Morphotropic phase boundary and electrical properties in $(1-x)Bi_{0.5}Na_{0.5}TiO_3$–$xBi(Zn_{0.5}Ti_{0.5})O_3$ lead-free piezoceramics, J. Appl. Phys. 107 (2010) 114110.
[9] S.T. Zhang, A.B. Kounga, E. Aulbach, H. Ehrenberg, J. Rödel, Giant strain in lead-free piezoceramics $Bi_{0.5}Na_{0.5}TiO_3$–$BaTiO_3$–$K_{0.5}Na_{0.5}NbO_3$ system, Appl. Phys. Lett. 91 (2007) 112906.
[10] S.E. Park, T.R. Shrout, Ultrahigh strain and piezoelectric behaviour in relaxor based ferroelectric single crystal, J. Appl. Phys. 82 (1997) 1804–1811.
[11] H. Maiwa, S.H. Kim, N. Ichinose, Temperature dependence of the electrical and electromechanical properties of lead zirconate titanate thin films, Appl. Phys. Lett. 83 (2003) 4396–4398.
[12] S.T. Zhang, A.B. Kounga, E. Aulbach, W. Jo, T. Granzow, H. Ehrenberg, J. Rödel, Lead-free piezoceramics with giant strain in the system $Bi_{0.5}Na_{0.5}$-TiO_3–$BaTiO_3$–$K_{0.5}Na_{0.5}NbO_3$. II: temperature dependent properties, J. Appl. Phys. 103 (2008) 034108.
[13] S.T. Zhang, A.B. Kounga, E. Aulbach, T. Granzow, W. Jo, H.-J. Kleebe, J. Rödel, Lead-free piezoceramics with giant strain in the system $Bi_{0.5}Na_{0.5}$-TiO_3–$BaTiO_3$–$K_{0.5}Na_{0.5}NbO_3$. I: structure and room temperature properties, J. Appl. Phys. 103 (2008) 034107.
[14] S.T. Zhang, A.B. Kounga, E. Aulbach, Y. Deng, Temperature dependent electrical properties of $0.94Bi_{0.5}Na_{0.5}TiO_3$–$0.06BaTiO_3$ ceramics, J. Am. Ceram. Soc. 91 (2008) 3950–3954.
[15] G.A. Samara, The relaxational properties of compositionally disordered ABO_3 perovskites, J. Phys. Condens. Matter 15 (2003) R367–R411.
[16] R.P. Brodeur, K.W. Gachigi, P.M. Pruna, T.R. Shrout, Ultra-high strain ceramics with multiple field-induced phase transitions, J. Am. Ceram. Soc. 77 (1994) 3042–3044.
[17] S.E. Park, M.J. Pan, K. Markowski, S. Yoshikawa, L.E. Cross, Electric field induced phase transition of antiferroelectric lead lanthanum zirconate titanate stannate ceramics, J. Appl. Phys. 82 (1997) 1798–1803.
[18] Y.M. Chiang, G.W. Farrey, A.N. Soukhojak, Lead-free high-strain single-crystal piezoelectrics in the alkaline-bismuth–titanate perovskite family, Appl. Phys. Lett. 73 (1998) 3683–3685.